nature portfolio

https://doi.org/10.1038/s41928-021-00636-3

Supplementary information

Room-scale magnetoquasistatic wireless power transfer using a cavity-based multimode resonator

In the format provided by the authors and unedited

Supplementary information

Room-scale magnetoquasistatic wireless power transfer using a cavity-based multimode resonator

Takuya Sasatani[1*], Alanson P. Sample[2], and Yoshihiro Kawahara[1]

[1] Department of Electrical Engineering and Information Systems, Graduate School of Engineering, The University of Tokyo, Bunkyo-ku, Tokyo, Japan

[2] Electrical Engineering and Computer Science Department, University of Michigan, Ann Arbor, Michigan, USA

(*Corresponding author)

Email: sasatani@akg.t.u-tokyo.ac.jp

The equation and reference numbers refer to the main text unless otherwise specified.

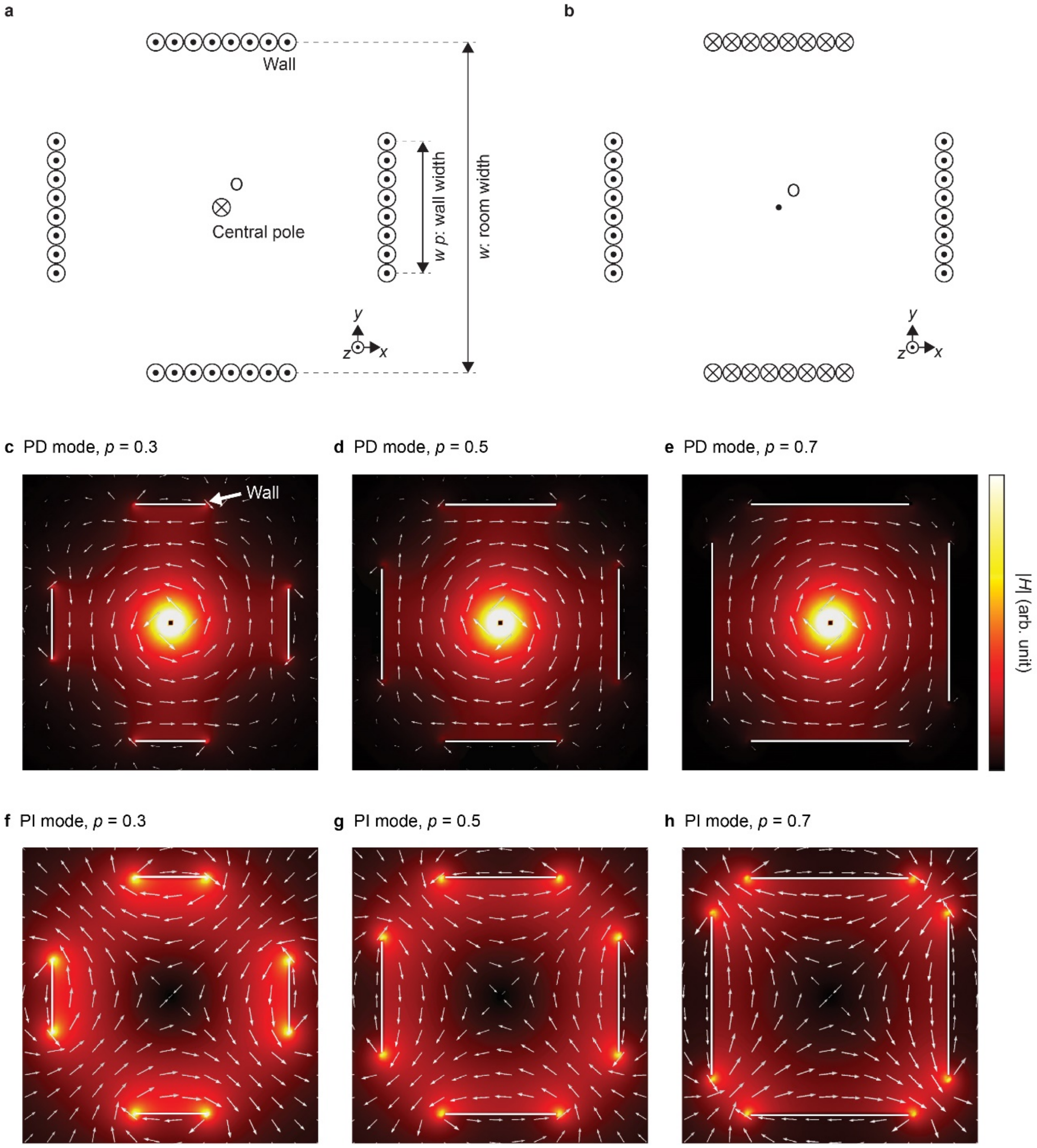

Supplementary Fig. 1. Top view of the current direction in the (**a**) Pole dependent (PD) mode and (**b**) Pole independent (PI) mode. Note that the ceiling and floor are omitted for simplicity. (**c-h**) Top view of magnetic field distributions with different wall width proportion *p* (see (**a**)).

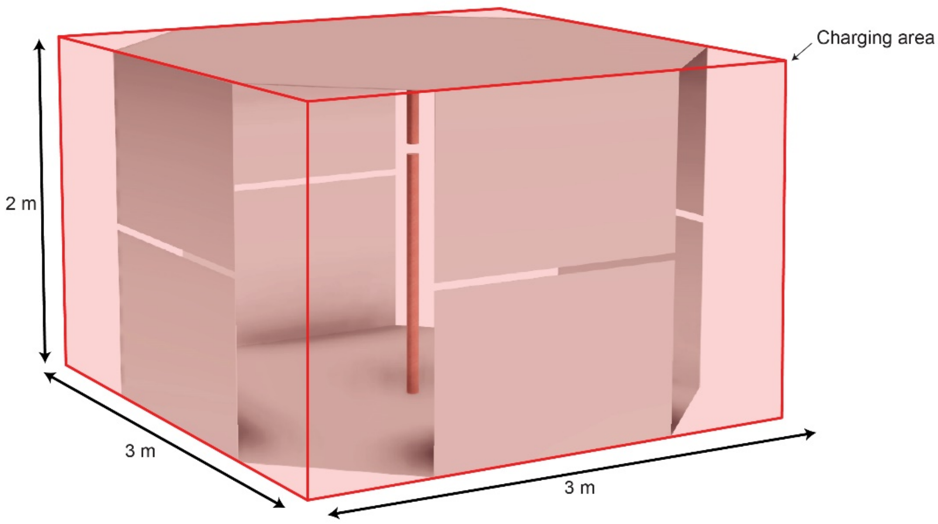

Supplementary Fig. 2. Charging area.

a

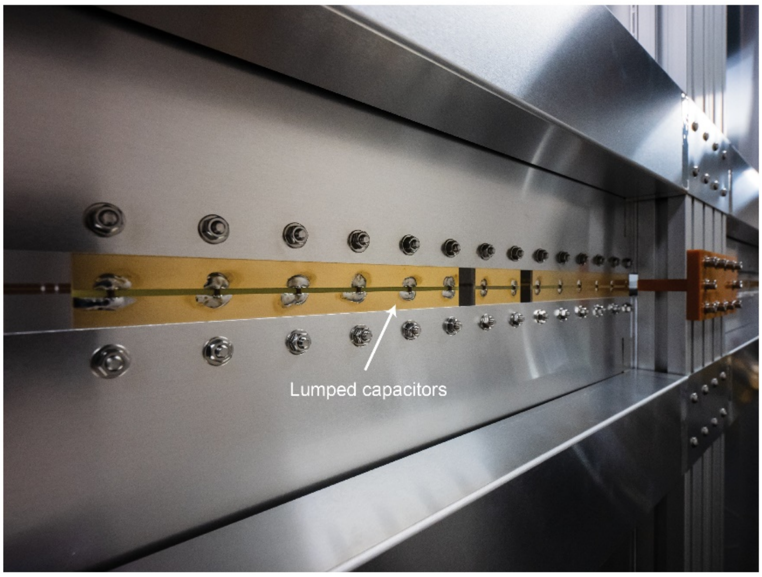

b

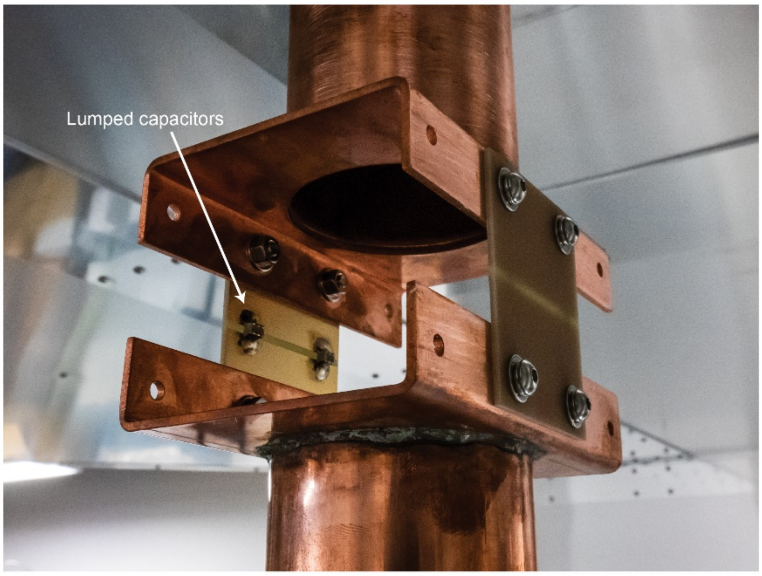

Supplementary Fig. 3. Capacitors mounted on the constructed room-scale resonator.

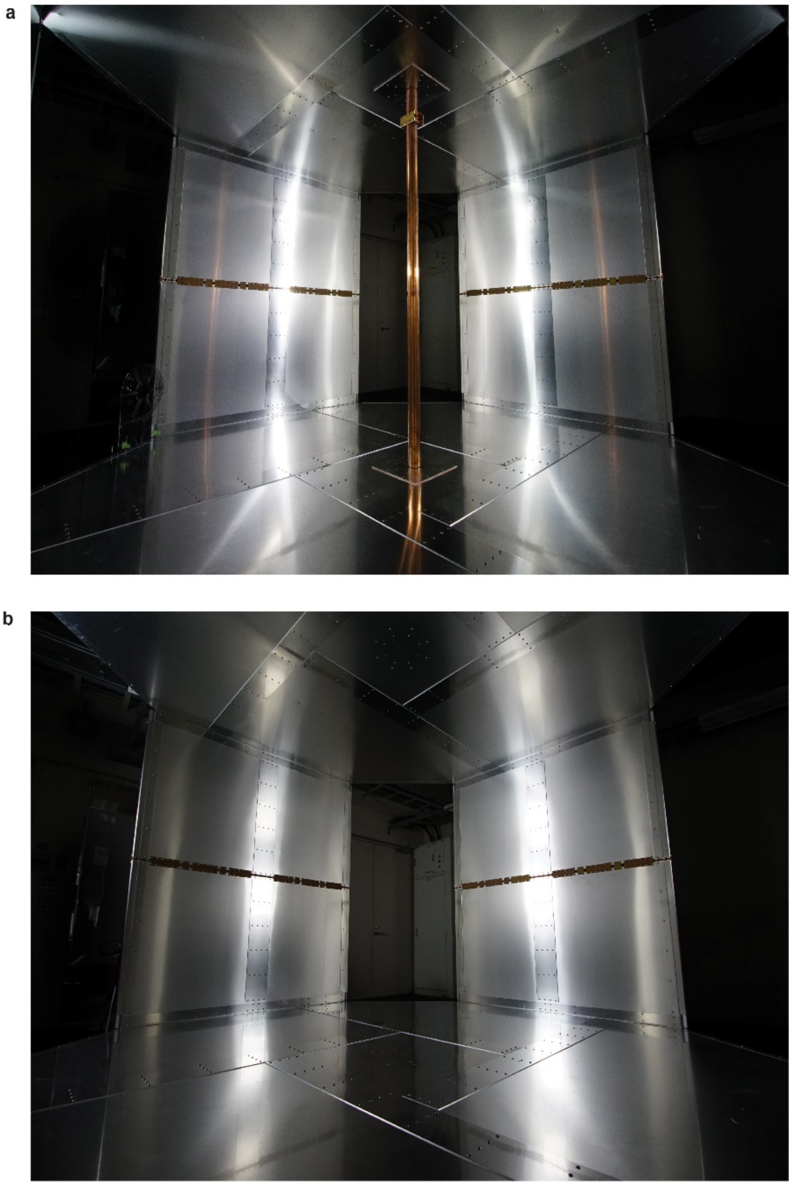

Supplementary Fig. 4. Internal view of the constructed M-QSCR (**a**) with the central pole and (**b**) without the central pole.

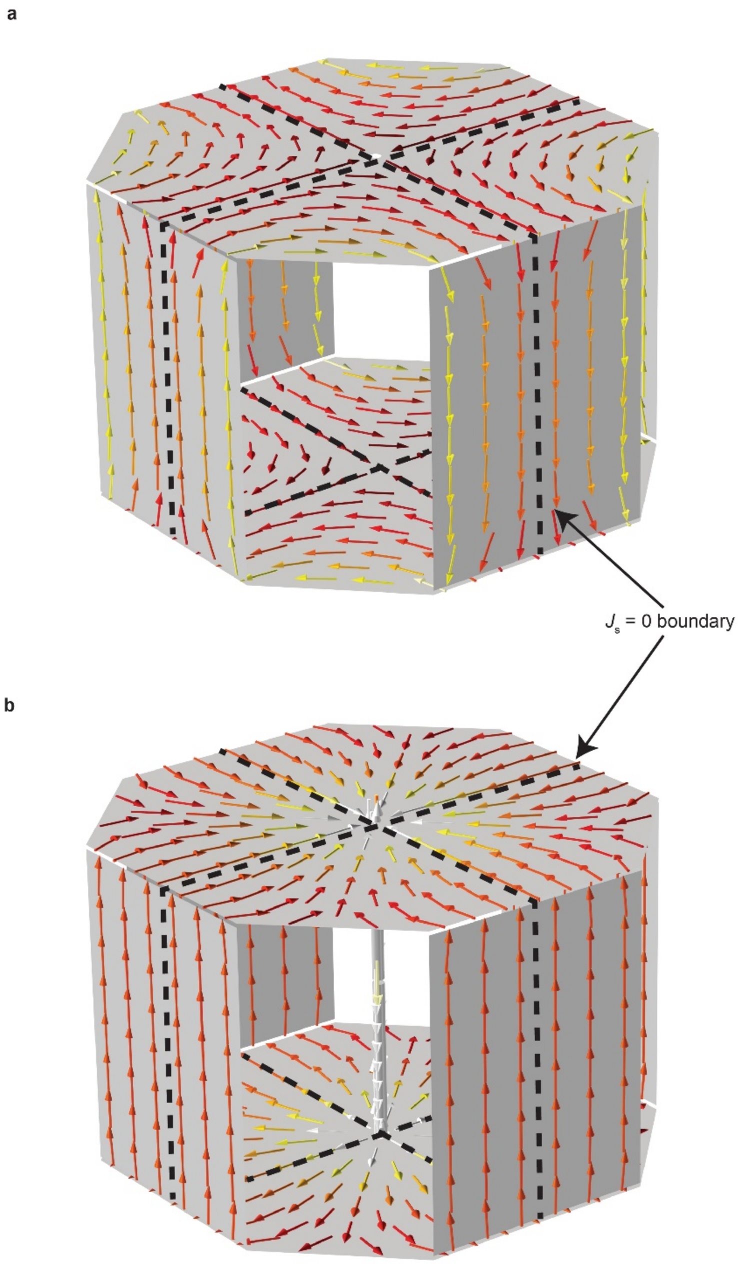

Supplementary Fig. 5. Current distribution in the (**a**) PI mode and (**b**) PD mode.

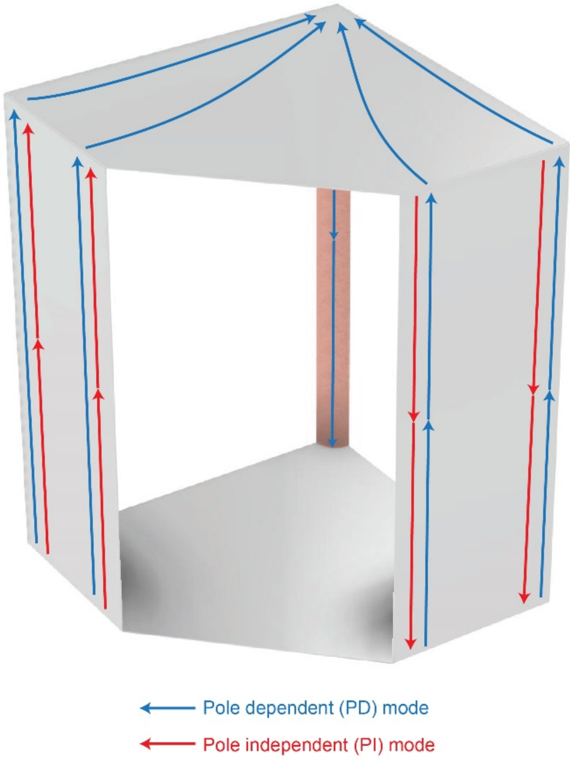

Supplementary Fig. 6. Unit structure (*i.e.* unit current loop) used for the analysis of resonant frequency. This is a quarter of the structure shown in Supplementary Fig. 5.

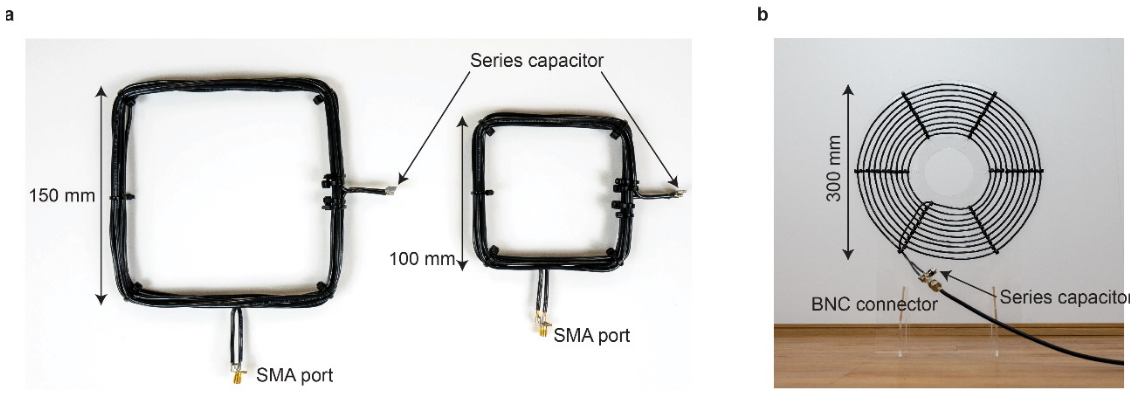

Supplementary Fig. 7. Coil resonators used in the measurements: (**a**) receiver coil and (**b**) drive coil.

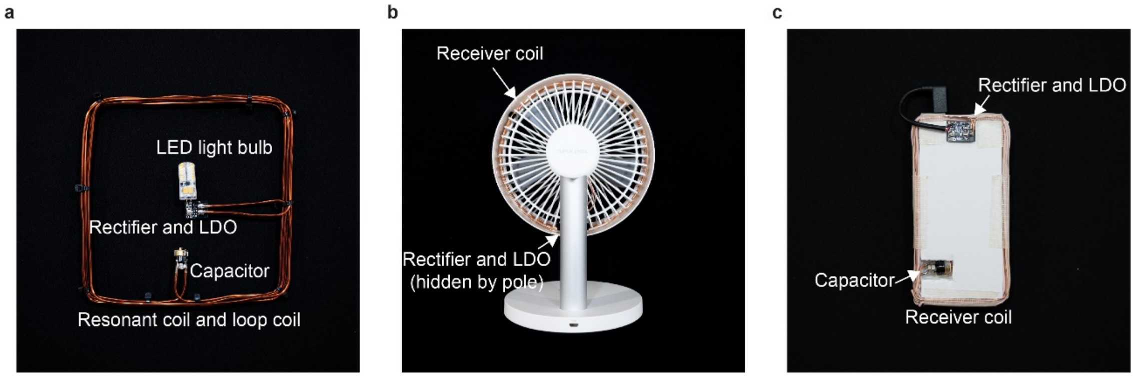

Supplementary Fig. 8. Electronic devices augmented with wireless power receivers: (**a**) light bulb in the floor lamp, (**b**) fan, and (**c**) back of a smartphone. The receivers are composed of a receiver resonator, a loop coil for impedance tuning, a full-bridge rectifier, a linear voltage regulator (LDO), and the load (*i.e.* the powered device).

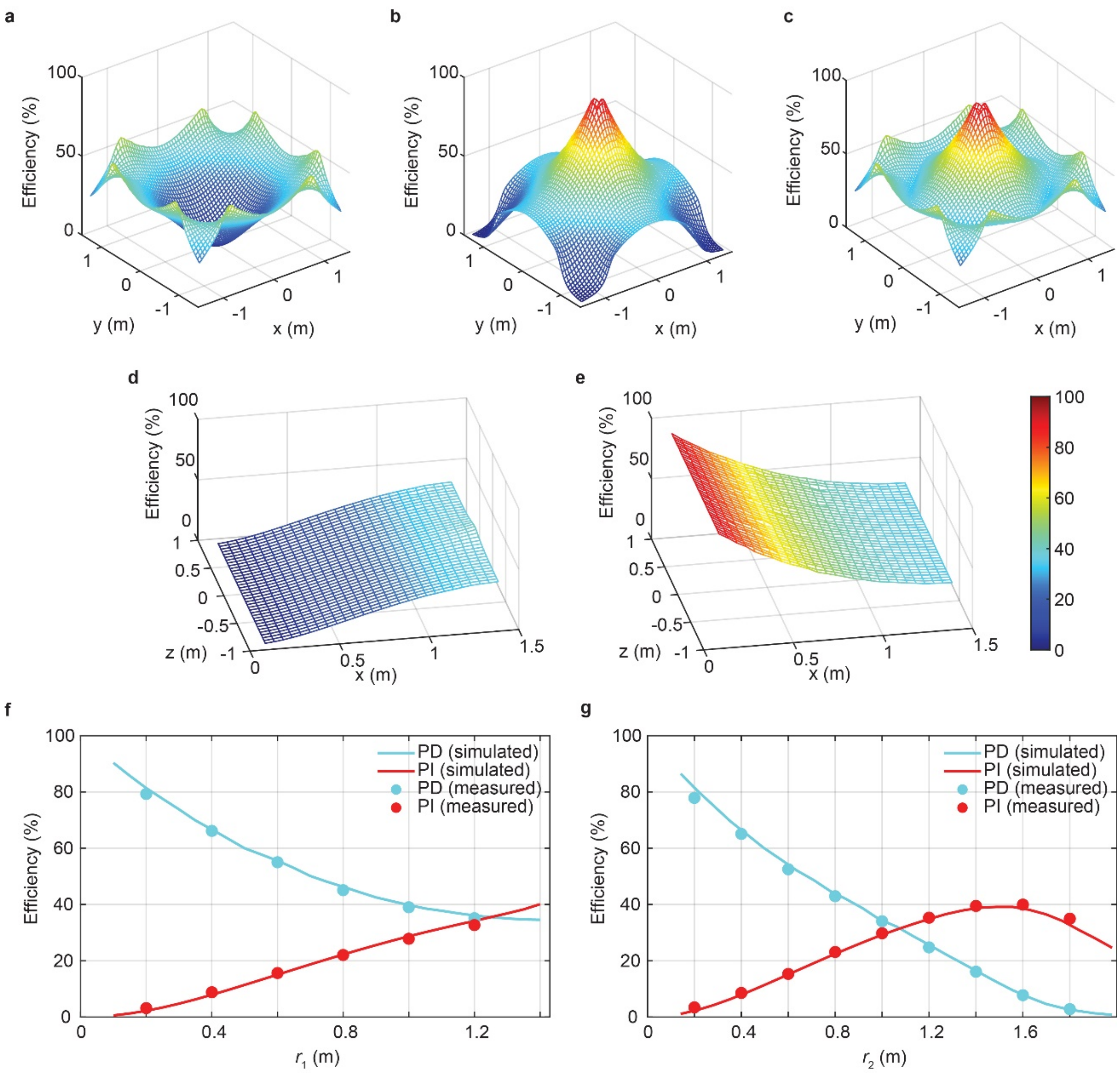

Supplementary Fig. 9. Evaluation of power transfer efficiency using a 100 mm square receiver coil. Efficiencies when the receiver is placed on the $z = 0$ plane (see Fig. 3 (**f**)) using the (**a**) pole independent (PI) mode, (**b**) pole dependent (PD) mode, and (**c**) both modes are shown. The power transfer efficiencies when the receiver is placed on the $y = 0$ plane using the (**d**) PI mode and (**e**) PD mode are shown. (**f**) shows the simulated and measured power transfer efficiency when the receiver is placed on line (i) (see Fig. 3 (**f**)). (**g**) shows the simulated and measured efficiencies when the receiver is placed on line (ii) (see Fig. 3 (**f**)).

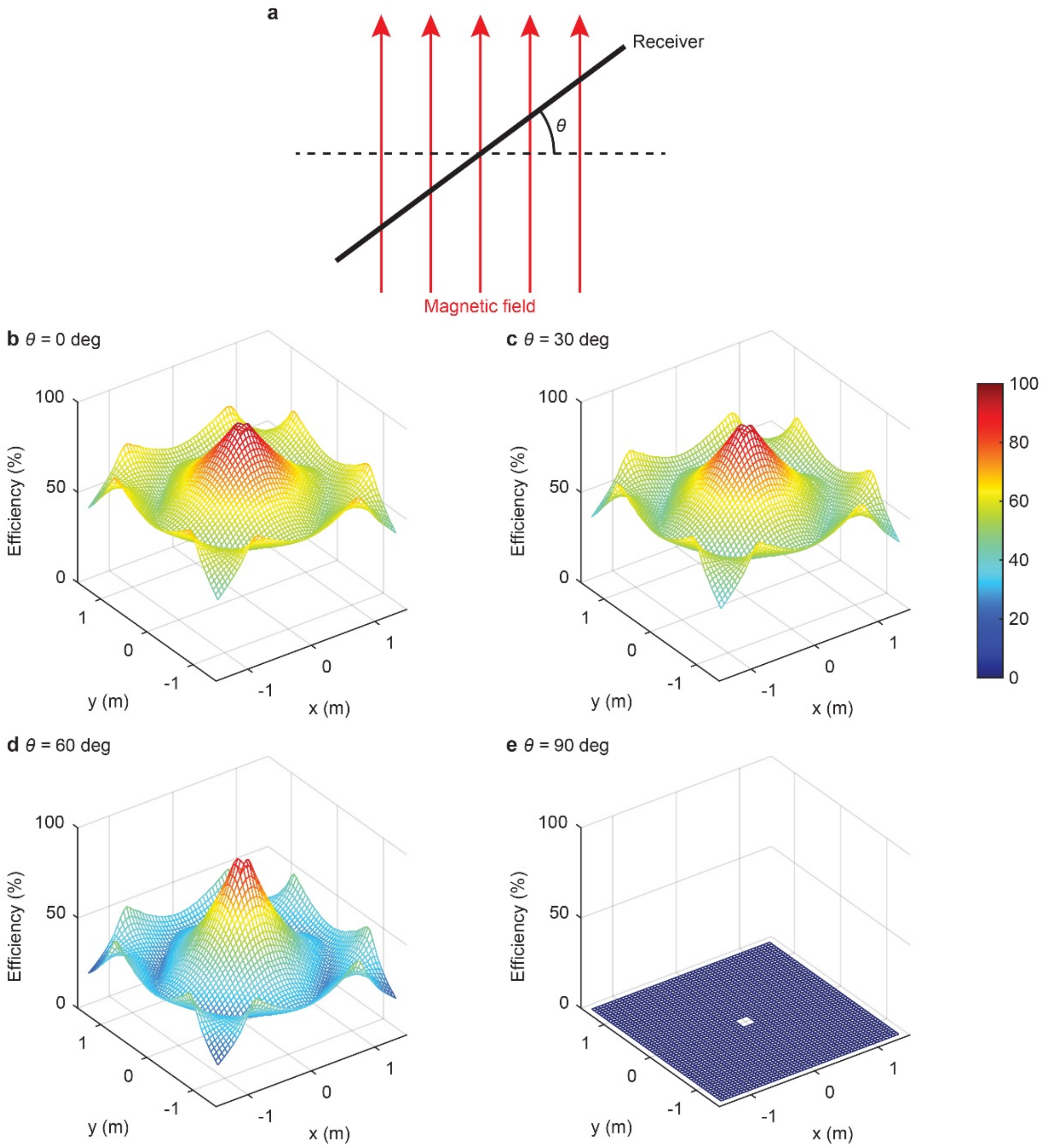

Supplementary Fig. 10. Evaluation of the power transfer efficiency using a misaligned receiver coil. (**a**) Definition of the misalignment angle θ. The efficiencies when (**b**) $\theta = 0°$, (**c**) $\theta = 30°$, (**d**) $\theta = 60°$, and (**e**) $\theta = 90°$ are shown.

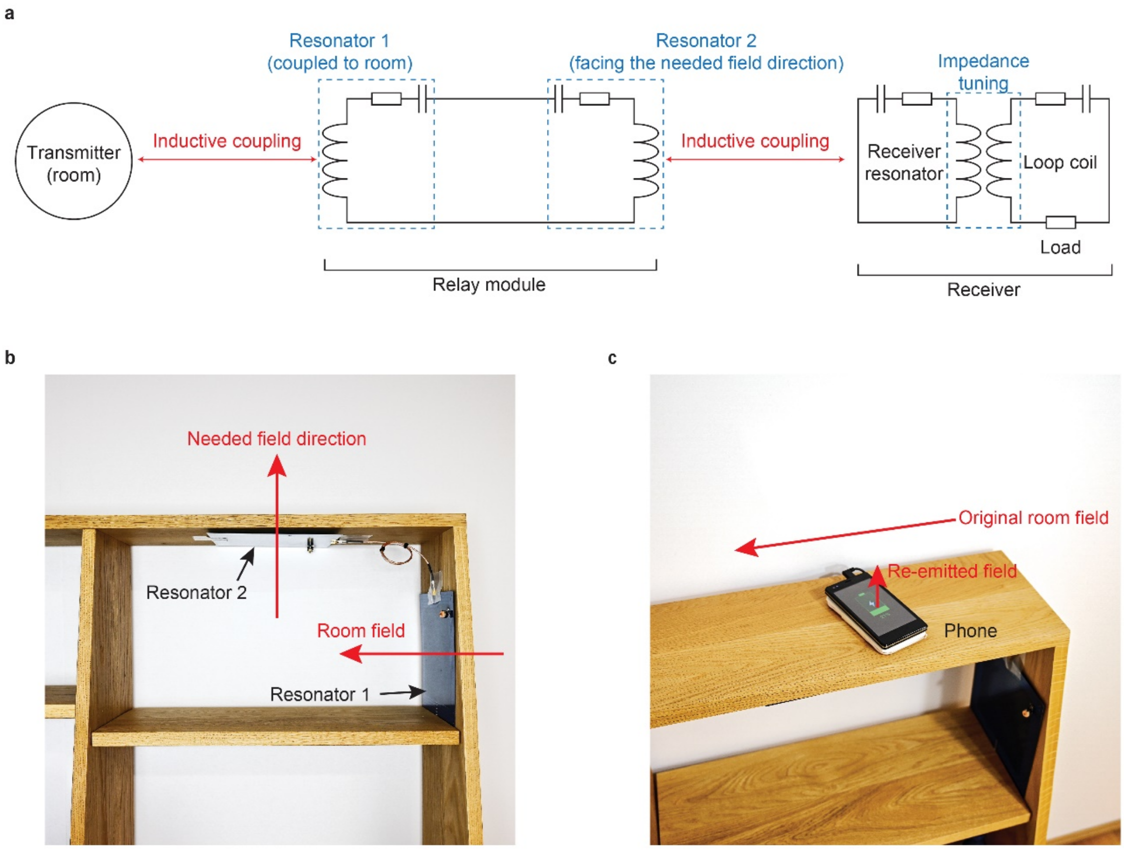

Supplementary Fig. 11. Example of using relay resonators for compensating for the orientation misalignment of the receiver. (**a**) System diagram. (**b**) Placement of the relay module. (**c**) Proof-of-concept demonstration of charging a phone on a shelf.

Supplementary Table 1. Comparison with other approaches.

	Previous approaches			Proposed approach
	Coil resonator (2-D array)	Cavity resonator[21, 22]	QSCR[19]	Multimode QSCR
Coverage	✗ Surface	✓ Full volume	✗ Biased to the centre[A]	✓ Full-volume[A]
Interaction with dielectrics (*e.g.* human, daily objects)	✓ Small	✗ Large	✓ Small	✓ Small
Resonant frequency tuning	✓ Adjustable	✗ Fixed by cavity dimention	✓ Adjustable	✓ Adjustable

[A] Simulations in ideal setups show that the minimum power transfer efficiency throughout the volume using the single-mode QSCR is 6%, whereas the multimode QSCR shows a minimum of 66% efficiency[23]. These analyses assume a 4.9 m × 4.9 m × 2.3 m room-scale transmitter and a 165 mm square coil receiver.

Supplementary Note 1. Effect of varying receiver size and orientation

Variations in the receiver coil size and orientation impact the coupling coefficient between the transmitter (*i.e.* room) and receiver, which determine the power transfer efficiency, as introduced in Methods. We note that the coil size also impacts the Q-factor. However, we consider discussing the relationship between coil size and Q-factor is beyond the scope of this study because it involves the application-specific optimisation of coil parameters, making it difficult to offer a general discussion.

The coupling coefficient could be computed using equations (7–9). Because the room-scale transmitter is significantly larger than the receiver, the field near the receiver is approximately uniform. Under this approximation, the captured flux β (see equation (9)) will be proportional to the receiver's cross-sectional area. Meanwhile, when the coil orientation varies by angle θ from the orientation where the normal vector and the magnetic field are aligned, it will introduce a $\cos\theta$ dependency on β. These two effects on β alter the coupling coefficient κ, according to equation (7). This, in turn, would impact the power transfer efficiency, as described in Methods.

To conclude this supplemental note, we present the evaluation of the power transfer efficiency under the following conditions: (i) when using a 100 mm square coil, which has a similar cross-sectional area with typical handheld mobile devices and (ii) when using a misaligned receiver coil. Supplementary Fig. 9 presents the results for (i). These results were obtained using the same measurement procedure as that for obtaining the results in Fig. 3. The measured Q-factor of the 100 mm square coil was 230. The power transfer efficiency exceeded 21.2% at any position within the room volume, which is lower than the efficiency of 37.1% achieved when using the 150 mm receiver. Supplementary Fig. 10 shows the efficiency when the receiver's normal vector is misaligned by angle θ. The 150 mm square receiver coil was used in this evaluation. The receiver was placed on the $z = 0$ plane (see Fig. 3 (**f**)), and both modes were used for power transfer. The efficiency decreased with the increase in misalignment and reduced to zero at $\theta = 90°$. Several potential approaches for compensating for this orientation misalignment are introduced in Supplementary Note 2.

Supplementary Note 2. Approaches for compensating for receiver orientation misalignment.

One limitation of this work (and previous works) is that the receiver needs to be placed in the appropriate orientation to capture a large amount of magnetic flux. However, once we extend the magnetic field to the area of interest, there are many potential approaches for addressing the receiver orientation issue, which could be selected based on the application's requirements. We briefly introduce two examples of such techniques herein. One well-known approach is to use multiple receiver coils[32,33]. Omnidirectional receivers could be achieved by combining multiple orthogonally oriented receivers, which capture the magnetic flux from different directions. Another potential method is to place passive relay modules within the powering area for "bending" the magnetic field. For instance, if we connect two resonant coils, where one couples with the room and the other faces the intended field direction, the relay would passively re-emit the field (see Supplementary Fig. 11). This "bending" effect could be turned ON and OFF by connecting a switch between the two relay resonators and connecting/disconnecting them. This approach will enable the remodelling of the field such that it seamlessly meets the space's affordance. A proof-of-concept demonstration of this approach is presented in Supplementary Fig. 11 (**b, c**).